Issues on Mechanical and Civil Engineering,
A Symposium to Honour Professor Enrique Alarcón
pp163-174
M Doblaré et al editors, UPM Press, Madrid, 2012.
ISBN: 978-84-939196-7-2

Coupled Models for the Dynamics of Bridges under High-Speed Rail Traffic

José M. Goicolea, Pablo Antolín
Escuela de Ingenieros de Caminos, Technical University of Madrid

Abstract

The dynamic effects of high-speed trains on viaducts are important issues for the design of the structures, as well as for determining safe running conditions of trains. In this work we start by reviewing the relevance of some basic moving load models for the dynamic action of vertical traffic loads. The study of lateral dynamics of running trains on bridges is of importance mainly for the safety of the traffic, and may be relevant for laterally compliant bridges. These studies require 3D coupled vehicle-bridge models and consideration of wheel to rail contact. We describe here a fully nonlinear coupled model, formulated in absolute coordinates and incorporated into a commercial finite element framework. An application example is presented for a vehicle subject to a strong wind gust traversing a bridge, showing the relevance of the nonlinear wheel-rail contact model as well as the interaction between bridge and vehicle.

1 Introduction

The dynamic behaviour of railway bridges under traffic loads has been an important consideration since the early days of railways in the 19th century, with significant implications both for the safety and the functionality of structures. The new high-speed trains introduce a potentially much greater dynamic effect, the resonant response of the bridge from regularly spaced axle loads at speeds whose effective frequency may coincide with the fundamental frequencies of the structure. Resonance is not adequately covered by an impact coefficient and requires a dynamic analysis of the bridge. As a result of research carried out in Europe to investigate high speed traffic actions [1] the new codes for design of railway bridges take into account resonant phenomena from traffic, ([2], [3]). These codes prescribe dynamic analyses to check resonance under certain circumstances.

The work on dynamics of railway bridges was pioneered in Spain by Enrique Alarcón, who focused his PhD thesis on this topic [4]. Soon after he published proposals for impact factors [5] and completed a comprehensive treatise on dynamics with Miguel A. Hacar [6]. This work served as the base for the 1975 spanish code for traffic actions on bridges [7]. In the early 80's and motivated by Enrique the first author became acquainted with new approaches to these problems of dynamics, taking advantage of the increasing availability of computers and new ideas such as the so-called *Component Element Method* [8]. Further innovations were published by Alarcón and co-workers [9]. Recent works compiling new developments in railway bridge dynamics have been published by Yang [10] and Xia et al. [11].

This paper also deals with the lateral dynamics of railway vehicles on viaducts, for which a 3D coupled full vehicle–structure interaction model must be employed. The interest for this study originates from the observation of significant lateral vibrations in some European railway bridges, with metallic open deck sections, high lateral compliance and consequently low lateral eigenfrequencies. These vibrations affect the train as well as the structure, and were studied under the auspices of ERRI [12]. A different type of railway structures with high lateral compliance in relative terms are the long continuous viaducts with high piers erected in some high-speed railway lines. Several such viaducts form part of the new Spanish HS lines [13].

In the rest of this paper we discuss first the dynamic response of bridges in section 2, reviewing the *"impact"* action of moving loads, resonance, and models available for dynamic analysis. Following, in section 3 we describe the models for lateral dynamics of vehicles on viaducts. A representative application will be presented in section 4. Finally, some concluding remarks are summarised in section 5.

2 Dynamic response of bridges

2.1 Dynamic response to a moving load

The dynamic response of a bridge under a moving load is a classical problem in structural dynamics. The basic solution for a simply supported bridge was already published in [14]. This solution provides a basis for defining a dynamic factor (or *impact factor*) for design.

From the dynamic equation of vibration of a beam, the solution may be developed with a modal analysis [14], in which we shall take only the fundamental mode of vibration of frequency $f_0 = \omega_0/2\pi$ (further down we shall consider the implications of taking more modes). For a load at constant speed v and a bridge of span L a non-dimensional parameter α for the load velocity may be defined as:

$$\alpha = \frac{\lambda}{2L} = \frac{v}{2f_0 L} \ . \tag{1}$$

The displacement time history response at the center of the span, in terms of the maximum static response $y_s = PL^3/48EI \approx 2PL^3/\pi^4 EI$ and considering some simplifications valid for small damping ($\zeta \ll 1$) may be expressed as:

$$y(t) = \frac{y_s}{1-\alpha^2}\left[\sin(\alpha\omega_0 t) - \alpha \mathrm{e}^{-\zeta\omega_0 t}\sin(\omega_0 t)\right] , \tag{2}$$

where the first term within the brackets is due to the excitation from the external load and the second to the free vibration of the bridge.

Figure 1 shows an application for a $L = 15$ m simply supported beam-type bridge, for speeds of 180 km/h and 360 km/h. The *impact factor* obtained is 1.2 in the first case and 1.7 in the second case. The solution in eqn (2) is valid during the time the load is on the bridge; under this assumption the maximum y_{dyn} in terms of t may be computed (for very fast moving loads when the maximum is reached after the load exits the bridge the response is lower). For the most unfavourable case without damping ($\zeta = 0$) the maximum is attained for $\dot{y} = 0 \ \Rightarrow \ \omega_0 t = \frac{2n}{1-\alpha}\pi$, resulting:

$$\frac{y_{\mathrm{dyn}}}{y_s} = \frac{1}{1-\alpha^2}\left[\sin\left(\frac{\alpha}{1-\alpha}2\pi\right) - \alpha \ \sin\left(\frac{1}{1-\alpha}2\pi\right)\right] \ . \tag{3}$$

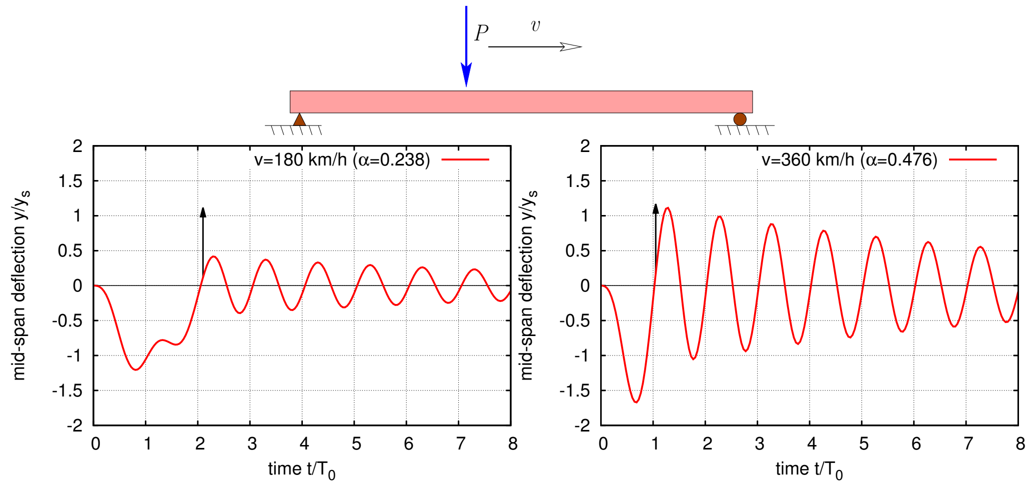

Figure 1: Response for a simply supported bridge ($L = 15$ m, $f_0 = 7$ Hz, $\overline{m} = 12$ t/m, $\zeta = 1.85\%$) for a moving load $P = 200$ kN at speeds of 180 km/h and 360 km/h. The arrow indicates for each case the time when the load exits the bridge and it continues under free vibrations. The axes represent in non-dimensional form the deflection relative to the static value $y(t)/y_s$ and the time relative to the fundamental period, t/T_0.

This expression yields an envelope of the dynamic factor with respect to the non-dimensional parameter α, plotted in figure 2. This envelope curve shows a maximum response for a critical value of α_c (and associated critical speed, $v_c = 2\alpha_c f_0 L$):

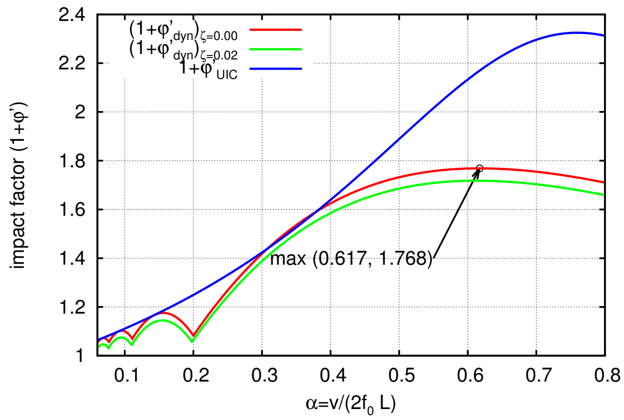

Figure 2: Envelopes of impact coefficient for moving load on bridge; φ'_{dyn} from analytic solution (3) and φ'_{UIC} from [15]. The various lobes in φ'_{dyn} correspond to slow loads for which the beam performs more than one full oscillation during passage.

$$\alpha_c = 0.617 \quad \Rightarrow \quad \left(\frac{y_{\text{dyn}}}{y_s}\right)_{\max} = (1 + \varphi'_{\text{dyn}})_{\max} = 1.768\,. \tag{4}$$

In figure 2 the envelope φ'_{UIC} from code [15] is also plotted for comparison, which proves to be sufficiently conservative. As an example, for the bridges in the D214 ERRI study [1] the maxima of φ'_{dyn} correspond to $v_c = 333\ \mathrm{km/h}$ for the $L = 15\ \mathrm{m}$ bridge and $v_c = 356\ \mathrm{km/h}$ for $L = 20\ \mathrm{m}$, velocities which may be attained by modern high-speed trains.

2.2 Dynamic analysis with moving loads

The regular patterns in axle spacings of trains may produce resonance in bridges, increasing greatly the dynamic effects from the impact effects of a moving load. For railway bridges these resonant effects appear in practice for speeds above 200 km/h. This requires a dynamic analysis for bridges in high-speed railway lines, which was not generally necessary for conventional railway lines with lower train speeds.

Figure 3 shows some measured results for a bridge in the Madrid-Sevilla HS line, from an AVE S100 (ALSTHOM) train at 220 km/h.

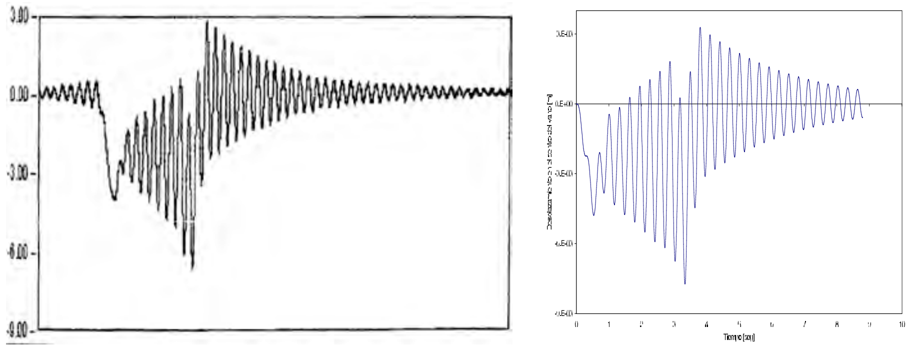

Figure 3: Measured vertical displacement at center of simply-supported span in viaduct over Tajo river, Madrid-Sevilla high-speed line, together with results of simulation with moving load model [16]. AVE S-100 single unit train at 220 km/h.

The bridge consists of a sequence of simply supported spans with $L = 38\ \mathrm{m}$. The measured and computed results show an impact coefficient of approximately $(1 + \varphi'_{\mathrm{dyn}}) = 2.0$, measured with respect to the highest static effects due to the locomotive loads. The effect would have been even greater for a double unit train (approx. 400 m length). This dynamic effect is not so much a problem for the Ultimate Limit State (ULS) of the bridge, which in this case is covered by the safety margins embedded in the normative static vertical load envelope LM71 and the impact coefficient Φ employed for the design [2]. However, in this case the functionality of the bridge was impaired: vibrations induced in the catenary posts proved to be excessive and these had to be relocated into new positions. In other cases the resonant dynamic effects may be even of much greater magnitude, and must be therefore avoided in the design of bridges.

The basic models for dynamic analysis consider the whole train taking into account the complete load sequence (figure 3). A general solution procedure is to employ finite element (FE) software for the discretization in space of the dynamic equations. The only feature which is special for this case as compared to general structural dynamics problems is the adequate definition of the actions from the moving loads, which needs an ad-hoc preprocessing.

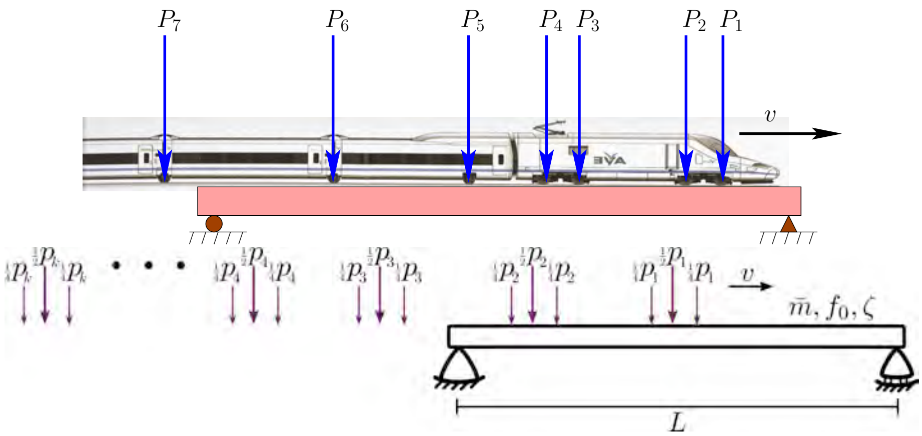

Figure 4: Model for moving load dynamic analysis. Top: load sequence for AVE S-102 (Talgo) HS train with regularly spaced single axles. Bottom: schematic view of model considering distribution of loads due to the track.

Two procedures exist for the solution in time: 1) a *direct time integration* of the coupled equations with a numerical scheme, or 2) a *modal analysis* of the discretised system obtaining numerical mode shapes and frequencies. These will then be available as uncoupled single degree of freedom equations and may be integrated in time individually. The modal analysis option has several advantages. The number of modes to consider can be chosen thus avoiding high-frequency components from higher modes, which are not significant for the bridge response. Moreover, the solution is generally much faster. The alternative approach of performing a direct time integration of the complete system provides a more general method, which may be necessary in some cases, for instance to consider nonlinear effects such as contacts. A particular case of interest is that of a straight beam subject only to vertical bending, for which the differential equation governing the dynamics is

$$\overline{m}\ddot{u} + (EI\ u'') = p(x,t) = \sum_{k=1}^{N} P_k \langle \delta(x + d_k - vt) \rangle \ , \tag{5}$$

for a train with N concentrated axle loads P_k with offsets d_k, where x is the longitudinal coordinate, $u(x)$ the beam vertical displacements, $\overline{m}$ the mass per unit length, and $\delta(\cdot)$ is the Dirac delta function. The brackets $\langle\cdot\rangle$ have the meaning $\langle \delta(\xi) \rangle = \delta(\xi)$ if $0 < \xi < L$ (load within bridge) or 0 otherwise. Superposed dots $(\dot{\bullet})$ represent time derivatives and primes $(\bullet\,')$ derivatives with respect to x. For simple cases, such as the simply supported beam, the spatial solution can be performed analytically through modal analysis, obtaining uncoupled modal equations for the amplitude of vibration of each mode.Considering mode shapes $\phi_i(x)$ and associated circular frequencies ω_i:

$$M_i \ddot{y}_i + 2\zeta_i \omega_i M_i \dot{y}_i \ \ + \omega_i^2 M_i y_i \ = \sum_{k=1}^{N} P_k \langle \phi_i (x + d_k - vt) \rangle, \tag{6}$$

where y_i is the amplitude for mode ϕ_i, M_i is the corresponding modal mass and ζ_i the damping ratio. These equations may be integrated in time by direct numerical algorithms (either coded directly or available within finite element software).

An issue which may be of importance is the number of modes to consider in the modal analysis. For a displacement analysis of a simply supported beam, it may be generally carried out with only the first (fundamental) mode. Acceleration analysis or the extraction of stresses or sectional resultants will often require more modes to be considered.

As an example, we present comparative results for the case of the ERRI D214 $L = 30$ m bridge under the ICE3 HS train in figure 4. The fundamental (first symmetric) mode frequency is in this case $f_1 = 3$ Hz, and the second symmetric mode is $f_3 = 27$ Hz (the 2$^{\mathrm{nd}}$ mode is skew-symmetric and has no influence on mid-span deflections). The analysis is performed here for a resonant velocity. It is clear from figure 4 (left) that for displacements only the fundamental mode is significant. However, a noticeable influence is seen in figure 4 (right) for accelerations from the second symmetric mode. Additional modes or even the direct integration with the complete model yield only minor increases to these accelerations.

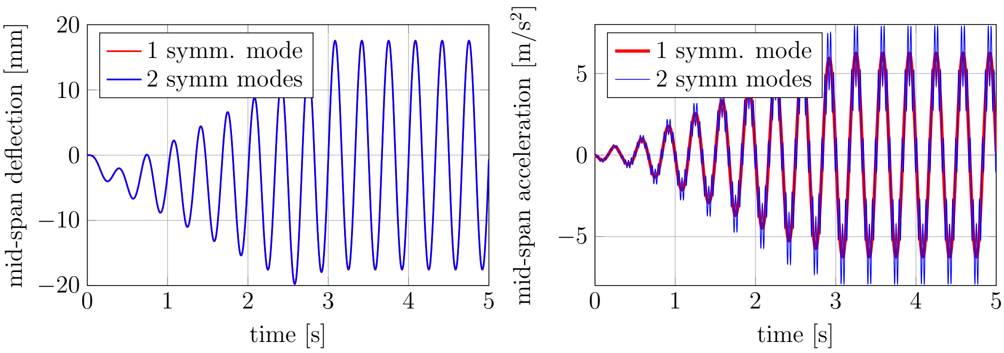

Figure 5: Influence of number of modes for simple bridge, on displacements and accelerations. ICE3 HS train at $v = 268$ km/h on $L = 30$ m bridge from ERRI D214 [1].

3 Lateral dynamics of vehicles on bridges

3.1 General features of model

The consideration of lateral dynamics for the response of railway vehicles on bridges requires three dimensional models, including degrees of freedom for lateral displacement, rolling and yawing in the vehicles. It is also necessary to employ coupled vehicle-structure models, which must take into account such features as nosing motion of wheelsets on the rails as well as track alignment irregularities. These features give rise to substantially more complex models than those used for vertical dynamics described in the previous section.

A fully nonlinear coupled model is proposed here for the lateral dynamic analysis of vehicles on viaducts. Vehicles are considered as three-dimensional multibody systems, and the bridge structure is modelled by means of finite elements. The model is developed in a general and modular way so that it may be easily implemented within an existing finite element analysis software with multibody capabilities. For this work Abaqus [17] finite element framework has been used. Both subsystems (bridge and vehicles) are described with coordinates in absolute reference frames, as opposed to alternative approaches which describe the multibody system with coordinates relative to the bridge motion at the base of the vehicle. This facilitates the full consideration of nonlinear inertia terms, without introducing additional difficulties for the structural mechanical behaviour [18]. Contrary to the majority of existing models for train–bridge dynamic interaction, the formulation described here is capable of full consideration of geometrical and material nonlinearities both in the structural subsystem (bridge) and in the multibody subsystem (vehicle). The approach for wheel–rail geometrical interaction and mechanical contact model is fully nonlinear as well, not being limited neither to constant conicity assumptions nor to linearized elastic contact forces.

The treatment of wheel to rail contact is based on the elastic contact forces approach [19]. The approach for contact point determination at each wheel employs a contact point determination based on a pre-computed geometric lookup table. A single hertzian contact point is considered at each wheel. Following the basic features of the model are summarised, for a more detailed description see [20].

3.2 Kinematics of wheelset and track

The wheelsets are considered as rigid bodies, within the vehicle multibody subsystem. The bridge deck cross sections are also assumed to be rigid within the structural finite element model, i.e. no distortion of the plane cross section is considered. This assumption is automatically enforced by standard 3D beam-type finite elements. However, both vehicle and bridge can undergo large displacements and rotations. In order to establish the contact interface with sufficient precision a detailed description of the positions and velocities of the wheel and rail points is required, whose key concepts are summarised below. A more general description of multibody kinematics for railway applications in [21].

We consider a bridge deck section at a position on the deck defined by the longitudinal coordinate s_w (Figure 6). The position vector of a point C on the rail may be expressed as

$$\mathbf{r}_C = \mathbf{r}_b + \mathbf{\Lambda}_b \widetilde{\boldsymbol{\rho}}_t + \mathbf{\Lambda}_t \overline{\boldsymbol{\rho}}_C \tag{7}$$

where $\mathbf{r}_b$ defines the position of the reference point on the deck section. Two reference frames are used for the track: the bridge section reference system $\{b, \mathbf{e}_i^b\}$ which is attached to the deck section at point b, and the track reference frame $\{t, \mathbf{e}_i^t\}$ attached to the track point t located at the mid point between the top of both rails and at the same deck section. $\mathbf{\Lambda}_b$ and $\mathbf{\Lambda}_t$ are, respectively, the rotation tensors that relate both reference systems and the inertial frame. The position of deck section reference point $\mathbf{r}_b$ and the rotation $\boldsymbol{\theta}_b$ are obtained by consistent interpolation of the finite element nodal degrees of freedom along the bridge deck.

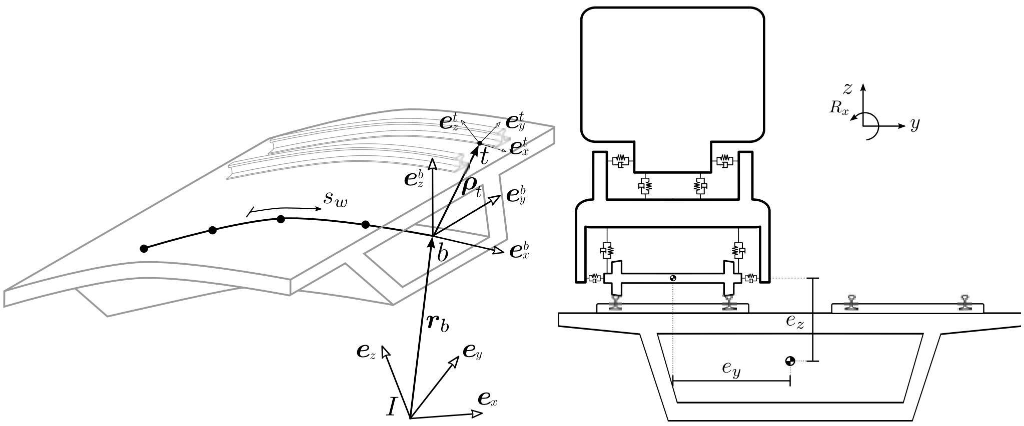

Figure 6: Reference frames and vectors for track kinematics: intermediate frame attached to the deck section $\{b, \mathbf{e}_i^b\}$ and the track coordinate system $\{t, \mathbf{e}_i^t\}$

3.3 Wheelset-track interaction

The contact forces between wheels and rails are computed in three consecutive stages:

1. *Contact* geometry: determine of the position of the wheelset considering realistic rail and wheel profiles ([20] for details);
2. Normal contact: following Hertz contact theory [22], obtain the dimensions and shape of the contact area (ellipse) and the normal stress distribution;
3. Tangential *contact:* compute the resultant forces and moment of the tangential stresses which appear as a consequence of the rolling contact.

Assuming that the material properties of wheel and rail are the same (material symmetry), the normal and tangential problems may be considered uncoupled [23] and solved sequentially after the determination of the contact geometry.

The solution for the tangential contact forces at each wheel contact is a key feature of the coupled model. This is obtained here using the *FastSim* algorithm [24], which involves a compromise between accuracy and computational cost. The FastSim method has been implemented by the authors [25] as a user subroutine within Abaqus [17].

For a given friction coefficient μ, the input variables for evaluation of tangential rolling forces are the the normal stress distribution, the ellipse semiaxes and the *creepages*, defined as $\xi = \left[\xi_x, \xi_y, \xi_r\right]^{\mathrm{T}}$ which are defined as:

$$\xi_{\{x,y\}} = \frac{(\mathbf{v}_A - \mathbf{v}_C)\cdot\mathbf{e}^c_{\{x,y\}}}{v} \qquad \xi_r = \frac{(\boldsymbol{\omega}_w - \boldsymbol{\omega}_t)\cdot\mathbf{e}^c_z}{v}, \tag{8}$$

with v the wheelset longitudinal velocity and $(\boldsymbol{\omega}_w, \boldsymbol{\omega}_r)$ the angular velocities of wheelset and track respectively. The FastSim model involves a discretisation in strips within the contact ellipse and integration along each strip, as shown in Figure 7. In this figure a representative case for distribution of tangential stresses is shown also.

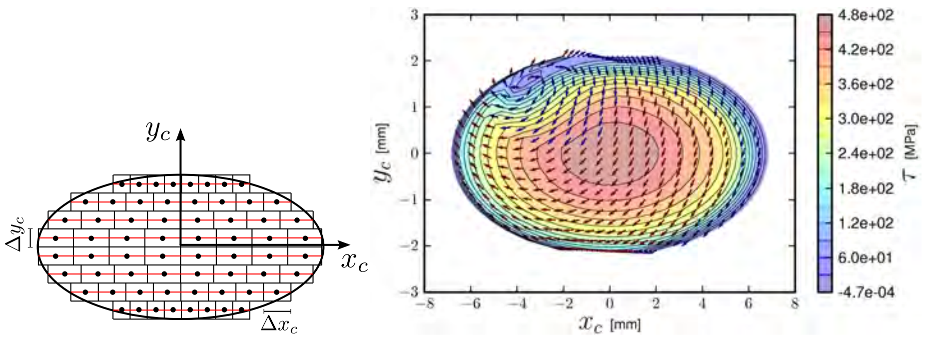

Figure 7: Discretisation of contact ellipse with FastSim and evaluation of tangential forces in rail-wheel contact

The resultants of the shear stress distribution at a point A are the forces T_x and T_y and the moment M_z whose directions are, respectively, $\mathbf{e}^c_x$, $\mathbf{e}^c_y$ and $\mathbf{e}^c_z$:

$$\mathbf{f}_{C,A} = T_x\,\mathbf{e}^c_x + T_y\,\mathbf{e}^c_y + N\,\mathbf{e}^c_z\,, \tag{9}$$

$$\mathbf{m}_{C,A} = M_z\,\mathbf{e}^c_x\,. \tag{10}$$

3.4 Vehicle-bridge system dynamics

Considering wheelset contact forces and moments from (7) $(\mathbf{f}_C, \mathbf{m}_C)$, applied external loads $(\mathbf{f}_E, \mathbf{m}_E)$ and loads transmitted by the suspension systems $(\mathbf{f}_S, \mathbf{m}_S)$, the Newton-Euler equations for a single wheelset can be written as

$$m\,\ddot{\mathbf{r}}_w + \mathbf{f}_S = \mathbf{f}_E + \mathbf{f}_C\,, \tag{11}$$

$$\mathbf{J}\,\dot{\boldsymbol{\omega}}_w + \boldsymbol{\omega}_w \times (\mathbf{J}\,\boldsymbol{\omega}_w) + \mathbf{m}_S = \mathbf{m}_E + \mathbf{m}_C\,, \tag{12}$$

being m the mass and $\mathbf{J}$ the inertia tensor for the wheelset.

Employing standard multibody dynamics models for the remaining of the vehicle, these equations may be assembled into a full system of equations for the complete vehicle. On the other hand, the discretised equations for the bridge structural dynamics may be obtained following standard finite element procedures, and expressed in a similar fashion.

The nonlinear set of coupled differential equations is solved in time using an implicit integration HHT-α algorithm, included in Abaqus [17]. This method has a good stability and robustness for the coupled problems described, and includes an inherent tunable numerical damping for the high frequency noise. The constraints inherent to the multibody subsystem are solved efficiently with augmented lagrangian procedures.

4 Application: wind gust on vehicle on continuous deck bridge

As a representative application, the response of a high-speed vehicle when it crosses over a multi-span bridge with continuous deck is analysed. The mechanical data for the vehicle are detailed in [20].

The structure is a single track continuous bridge consisting of six equal spans of $L = 50$ m each. The bridge is supported on two end abutments and five intermediate piers. Torsional rotation is allowed at the piers but constrained at the abutments. The deck cross section properties are uniform along the bridge length, see [20]. The first lateral and vertical bending eigenfrequencies are equal, of value 2.18 Hz; the first torsion eigenfrequency is 1.10Hz. Euler-Bernoulli beam elements of 1m length with linear elastic behaviour have been used.

The vehicle runs at a constant velocity of 100 km/h, with a lateral transient wind gust load defined by a chinese hat function [26] applied, with maximum value $F_{\max} = 270$ kN and gust duration $\tau = 0.1$ s (Figure 8). This load is applied on the vehicle car-body along y direction (transversal) when the last wheelset of the vehicle enters the bridge.

In Figure 9 the lateral response of the last wheelset of the vehicle when it crosses the bridge is shown, compared with the case for a perfectly rigid track (i.e. no structure). It can be seen that wheel flanges contact the lateral part of rail heads, the limits are indicated in the graph with dotted lines. We remark that for assessment of these running safety scenarios a nonlinear model such as proposed here is essential, as linear models cannot reproduce wheel–flange impacts.

Figure 10 shows the lateral response of the vehicle car-body and Figure 11, the tangential force T_y time history. This force is expressed at each instant in the local tangent plane to the wheel contact (i.e. frame $\{C,\ \mathbf{e}_i^c\}$) of the left wheel of the last vehicle wheelset; it cannot be interpreted as a lateral load.

Figure 9 shows a significantly different response for wheelset displacements when the structure flexibility is taken into account: not only in terms of amplitude of oscillations, but also of frequency. A similar remark can be made for the car-body displacements, Figure 10. Moreover, contact forces in Figure 11 exhibit peaks which correspond to the flange impacts, these impacts differ significantly in both models.

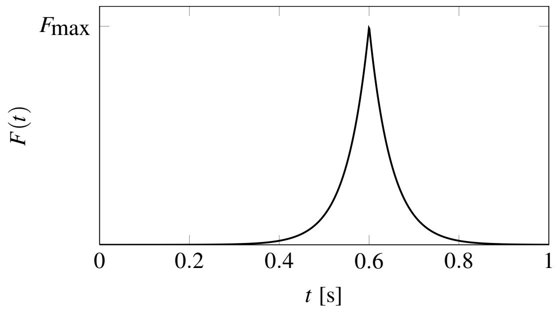

Figure 8: Lateral force history on vehicle car-body: wind gust load corresponding to a *"chinese hat"* function

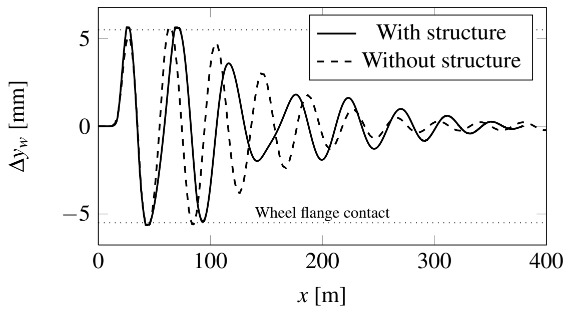

Figure 9: Lateral response of last wheelset; dotted lines indicate limit for wheel flange contact

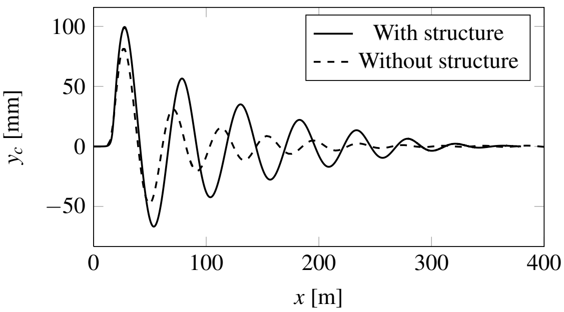

Figure 10: Lateral response of the car-body under an applied wind gust load

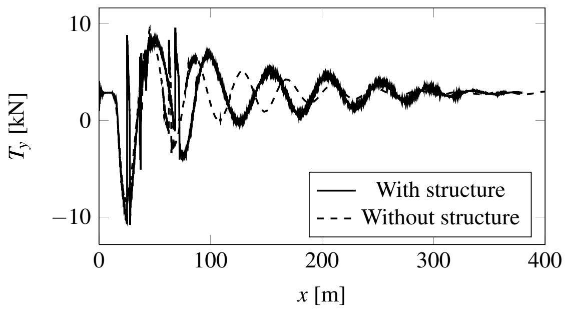

Figure 11: Tangential contact forces at the left wheel of the last wheelset, showing peaks for wheel–flange contact

5 Conclusion

The dynamic effects of high-speed trains on viaducts are important issues for the design of the structures, as well as for the consideration of safe running conditions of the trains, specially in high-speed railways.

The study of lateral dynamics of running trains on bridges is of importance mainly for the safety of the traffic on laterally compliant bridges, requiring 3D coupled vehicle-bridge models and consideration of wheel to rail contact. A fully nonlinear coupled model is proposed here, described in absolute coordinates and incorporated into a commercial finite element framework. The applications presented demonstrate the relevance of the coupling effect between vehicle and bridge, as well as for considering nonlinear contact wheel-rail models.

6 Acknowledgments

The authors are grateful for support from *Ministerio de Ciencia e Innovación* of Spanish Government in the project *Integración de la Monitorización de Viaductos Ferroviarios en el Sistema de Gestión y Mantenimiento de Infraestructuras "VIADINTEGRA"* (IPT-370000-20190-012), of the subprogram *INNPACTO*. The authors acknowledge also the support from the Technical University of Madrid, Spain.

7 References

[1] ERRI. *Committee D214 final report: Design of Railway Bridges for Speed up to 350 km/h; Dynamic loading effects including resonance*. European Railway Research Institute, Utrecht, The Netherlands, 1998.

[2] CEN. *EN1991-2:2003 Eurocode 1 – Actions on structures, Part 2: Traffic loads on bridges*. European Committee for Standardization, 2003.

[3] Ministerio de Fomento *IAPF-07: Instrucción sobre las acciones a considerar en el proyecto de puentes de ferrocarril*. Government of Spain, 2007.

[4] Alarcón, E. *Dinámica de puentes de ferrocarril*. Ph.D. thesis, Technical University of Madrid, 1970.

[5] Alarcón, E. El coeficiente de impacto en puentes de ferrocarril. *Revista de Obras públicas*, 1971.

[6] Hacar, M. & Alarcón, E. *Elementos de dinámica aplicada a las estructuras*. Edix,

Colegio de Ingenieros de Caminos, Canales y Puertos, 1971.
[7] Ministerio de Obras Públicas y Urbanismo *Instrucción relativa a las acciones a considerar en el proyecto de puentes de ferrocarril (IAPF-75)*. Government of Spain, 1975.
[8] Levy, S. & Wilkinson, J. *Component element method in structural dynamics*. McGraw Hill, 1976.
[9] Alarcón, E., Álvarez, R., Doblaré, M. & Molina, J. Efectos dinámicos en puentes de ferrocarril. *Hormigón y acero*, 1985.
[10] Yang, Y.B., Yau, J.D. & Wu, Y.S. *Vehicle-Bridge Interaction Dynamics: With Applications To High-Speed Railways*. World Scientific Publishing Company, Singapore, 1st edition, 2004. ISBN 9812388478.
[11] Xia, H., De Roeck, G. & Goicolea, J.M., editors. *Bridge Vibration and Controls: New Research*. Nova Science Publishers, 2012. ISBN 978-1-62100-868-2.
[12] ERRI. *Committee D181 final report: Forces Latérales sur les Ponts Ferroviaires*. European Railway Research Institute, Utrecht, The Netherlands, 1996.
[13] Millanes, F., Pascual, J. & Ortega, M. 'Arroyo de las Piedras' viaduct: The first composite steel-concrete high speed railway bridge in Spain. *Structural Engineering International*, **17**(4), 292–297, 2007.
[14] Timoshenko, S.P. *Vibration problems in engineering*. Van Nostrand, 1928.
[15] UIC. *Code UIC 776-1: Charges a prendre en consideration dans le calcul des ponts-rails*. Union Internationale des Chemins de Fer, 5 edition, 2006.
[16] Domínguez Barbero, J. *Dinámica de puentes de ferrocarril para alta velocidad: métodos de cálculo y estudio de la resonancia*. Ph.D. thesis, Technical University of Madrid, 2001. Http://oa.upm.es/1311.
[17] Simulia Ltd. *Abaqus 6.10 User's manual*. Providence, RI, 2010.
[18] Simo, J.C. & Vu-Quoc, L. The role of non-linear theories in transient dynamic analysis of flexible structures. *Journal of Sound and Vibration*, **119**(3), 487–508, 1987. doi:10.1016/0022-460X(87)90410-X .
[19] Shabana, A.A., Zaazaa, K.E., Escalona, J.L. & Sany, J.R. Development of elastic force model for wheel/rail contact problems. *Journal of Sound and Vibration*, **269**(1-2), 295–325, 2004. doi:10.1016/S0022-460X(03)00074-9 .
[20] Antolin, P., Goicolea, J.M., Oliva, J. & Astiz, M.A. Nonlinear train-bridge lateral interaction using a simplified wheel-rail contact method within a finite element framework. *Journal of Computational and Nonlinear Dynamics*, **7**(4), 1–18, 2012.
[21] Shabana, A.A., Zaazaa, K.E. & Sugiyama, H. *Railroad Vehicle Dynamics: A Computational Approach*. CRC Press, 2008.
[22] Hertz, H. Über die berührung fester elasticher körper and über die härtean. *J. für reine und agewandte Mathematik*, **92**, 156–171, 1882.
[23] Kalker, J.J. *Three-Dimensional Elastic Bodies in Rolling Contact (Solid Mechanics and Its Applications)*. Springer, 1990.
[24] Kalker, J.J. A Fast Algorithm for the Simplified Theory of Rolling Contact. *Vehicle System Dynamics*, **11**(1), 1–13, 1982. doi:10.1080/00423118208968684 .
[25] Antolin, P., Goicolea, J.M. & Astiz, M.A. Strategies for Modeling Train-Bridge Lateral Dynamic Interaction. In H. Xia, G. De Roeck & J.M. Goicolea, editors, *Bridge Vibration and Controls: New Research*, Nova Science Publishers, Inc., Hauppauge, NY, chapter 6, p. In press. 2012. ISBN 978-1-62100-868-2.
[26] CEN. *EN14067-6: Railway applications – Aerodynamics – Part 6: Requirements and test procedures for cross wind assessment*. European Committee for Standardization, 2010.